

# CrystEngComm

Accepted Manuscript



This is an *Accepted Manuscript*, which has been through the Royal Society of Chemistry peer review process and has been accepted for publication.

*Accepted Manuscripts* are published online shortly after acceptance, before technical editing, formatting and proof reading. Using this free service, authors can make their results available to the community, in citable form, before we publish the edited article. We will replace this *Accepted Manuscript* with the edited and formatted *Advance Article* as soon as it is available.

You can find more information about *Accepted Manuscripts* in the [Information for Authors](#).

Please note that technical editing may introduce minor changes to the text and/or graphics, which may alter content. The journal's standard [Terms & Conditions](#) and the [Ethical guidelines](#) still apply. In no event shall the Royal Society of Chemistry be held responsible for any errors or omissions in this *Accepted Manuscript* or any consequences arising from the use of any information it contains.



## Morphology-controlled assembly and enhanced emission of fluorescence in organic nanospheres and microrods based on 1,2-diphenyl-4-(4-dibenzothienyl)phenyl)-1,3-cyclopentadiene

Received 00th January 20xx,  
Accepted 00th January 20xx

DOI: 10.1039/x0xx00000x

www.rsc.org/

Junwei Ye,<sup>a</sup> Xueming Huang,<sup>a</sup> Yuan Gao,<sup>a</sup> Xiaoxiao Wang,<sup>a</sup> Ting Zheng,<sup>a</sup> Yuan Lin,<sup>a</sup> Xin Liu,<sup>\*b</sup> and Guiling Ning<sup>\*a</sup>

Fluorescent organic nanospheres, pod-like connecting spheres and microrods based on 1,2-diphenyl-4-(4-dibenzothienyl)phenyl)-1,3-cyclopentadiene (DPCP) have been prepared *via* controlling the solvent composition. The influence of concentration, surfactants and solvents on the morphologies of products was examined. The formation of particles with different morphology could be attributed to the solubility controlled crystalline nucleation. Single crystal X-ray analysis reveals the molecule of DPCP has non-coplanar geometry, and two molecules are packing to form a dimer as X-aggregates. Further, one-dimensional chain of DPCP additionally avoided the maximum face-to-face stacking. The solution of DPCP in methanol has weaker emission with a peak at 455 nm, however, the nanospheres, pod-like connecting spheres and microrods exhibit remarkably enhanced fluorescence emission with peaks at 447, 448, 468 nm, respectively. Additionally, fluorescent change behavior was further verified by DFT calculation and time-resolved emission decay measurements.

### Introduction

Organic micro/nanomaterials are the subject of intensive research due to their potential applications in many fields such as light-emitting devices, organic field effect transistors, photovoltaic cells, photocatalysis, drug delivery, bio-labeling and chemosensors.<sup>1-4</sup> Since H. Nakanishi and coworkers<sup>5</sup> demonstrated that perylene microcrystals showed different and size-dependent luminescent properties from those of bulk materials, self-assembly of fluorescent small organic molecules has attracted considerable research interest for their unique electronic and optical properties.<sup>6</sup> Particularly,  $\pi$ -conjugated organic molecule-based micro/nanomaterials are considered to be promising candidates for optical-related applications.<sup>7-9</sup> A number of methods including reprecipitation, solvent evaporation, physical/chemical vapor deposition, template-assisted growth and electrochemical deposition have been used to prepare most organic micro/nanostructures with different morphologies.<sup>10-12</sup> For example, microrods, nanowires and polyhedral microparticles of 9,10-diphenylanthracene<sup>13</sup>

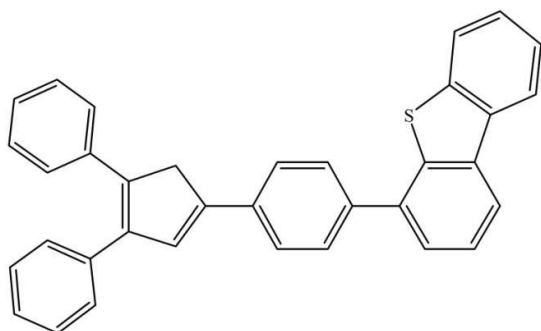
and 2,5,8,11-tetra-*tert*-butylperylene<sup>14</sup> were synthesized *via* a surfactant-assisted method, respectively. Particles of 4-amino-3-(2-(2-hydroxybenzylidene)hydrazinyl)-1H-1,2,4-triazole-5(4H)-thione with different crystal packing were fabricated in the presence or absence of water.<sup>15</sup> However, the morphology and size-controlled assembly of conjugated organic molecules and understanding of the formation mechanism of their aggregates is still a major challenge.

In our continuing research on the synthesis and fluorescent properties of conjugated organic molecules,<sup>16, 17</sup> we are interested in assembling micro/nanostructures of cyclopentadiene derivatives (CPDs) for their interesting aggregation induced emission enhancement (AIEE) property and promising application in photo- and electro-luminescent devices.<sup>18, 19</sup> Especially, morphology and size of the particles have a significant influence on the performance of CPDs. For example, Yao and co-workers reported crystalline 1,2,3,4,5-pentaphenyl-1,3-cyclopentadiene (PPCP) nanoribbon prepared using an adsorbent-assisted physical vapour deposition (PVD) method, which exhibited a fascinating multicolor emission properties.<sup>18</sup> Therefore, it is highly desirable to explore the facile approaches towards CPDs micro/nanostructures with different morphologies. Herein, we report the morphology-controlled assembly of a new cyclopentadiene derivative, 1,2-diphenyl-4-(4-dibenzothienyl)phenyl)-1,3-cyclopentadiene (DPCP) (Scheme 1). Fluorescent nanospheres and microrods of DPCP were easily obtained by solvent-induced assembly method.

<sup>a</sup> State Key Laboratory of Fine Chemicals and School of Chemical Engineering, Dalian University of Technology, 2 Linggong Road, Dalian 116012, P. R. China. E-mail: ninggl@dut.edu.cn. Fax: +86-411-84986065.

<sup>b</sup> College of Chemistry, Dalian University of Technology, 2 Linggong Road, Dalian 116012, P. R. China. E-mail: xliu.paper@gmail.com.

† Electronic Supplementary Information (ESI) available: SEM, FM, UV-vis absorption and photoluminescence spectra and crystallographic data (CCDC 1052063) in CIF or other electronic format See DOI: 10.1039/x0xx00000x



Scheme 1 Structure of DPCP.

## Experimental

### Materials and methods

All commercial chemicals were of analytical grade and were used without further purification. The samples were characterized by powder X-ray diffraction (PXRD, Rigaku-DMAX 2400) in reflection mode (Cu-K $\alpha$  radiation) with a  $2\theta$  scan in the range of 5–80°. The shapes and structures of samples were obtained with scanning electron microscope (SEM, Quanta-450, operated at 20 kV) and transmission electron microscopy (TEM, TecnaiF30, operated at 20 kV). All  $^1\text{H}$ - and  $^{13}\text{C}$ -NMR spectra were obtained using a Bruker AVANCE-400 MHz magnetic resonance spectrometer. HRMS were acquired on Micromass-GTC spectrometer. Fluorescence microscopy images were carried out with fluorescence microscope (OLYMPUS BX51). UV-Vis absorption measurements were conducted on HITACHI U-4100 UV-Vis Spectrophotometer. The photoluminescence (PL) studies were performed using a JASCO FP-6300 spectrofluorimeter with a 150 W Xe lamp. The relative fluorescence quantum yields were estimated relative to solutions of 0.05 mM quinine sulfate with  $\Phi_f = 0.55$  in 0.1 M sulfuric acid solution as a standard sample. Fluorescence lifetimes were measured with an Edinburgh Instruments OB920 fluorescence spectrometer.

### Synthesis

According to our previous works,<sup>17</sup> DPCP was synthesized by aldol condensation reaction then followed by Suzuki coupling reactions between 1,2-diphenyl-4-(4-bromophenyl)-1,3-cyclopentadiene and 4-dibenzothiénylboronic acid in the presence of  $\text{K}_2\text{CO}_3$  as base source and  $\text{Pd}(\text{PPh}_3)_4$  as catalyst (for details see ESI, Scheme S1). The solvent evaporation method was used to fabricate DPCP particles. In a typical procedure, a 50  $\mu\text{L}$  of DPCP in methanol solution with different concentration was dropped on a substrate located in a glass container with a cover. After evaporation of the solvents at room temperature, the monodispersed and pod-like connecting spheres were obtained on the substrate.

In order to investigate the effect of water on the morphologies of DPCP aggregates, 1.0 mL stock of 0.05 mM DPCP/methanol was injected into 4.0 mL of distilled water at room temperature. After vigorous stirring for 10 minutes and leaving the mixture to stand for 5 h, the solution containing

suspended nanoparticles was dropped on a glass-substrate in a container with a cover, and the microrods were obtained after evaporation of the solvents.

## Results and discussion

Fig. 1 shows the scanning electron microscopy (SEM) and fluorescence microscopy (FM) images of the DPCP particles with different morphology which were obtained by the solvent-induced assembly method *via* changing the solvent composition. As shown in Fig. 1a, monodispersed spheres with the size in the range of 300–500 nm were prepared on the substrate by using DPCP/methanol solution with a lower concentration of 0.01 mM. FM image revealed that the nanospheres have strong blue emission under UV irradiation (Fig. 1b). With the increase of concentration of DPCP/methanol solution, the size of spheres was increased and the bigger connecting spheres were obtained. When concentration was higher than 0.05 mM, the pod-like connecting spheres with the length of 1.5–3.5  $\mu\text{m}$  were formed together with some monodispersed spheres (Fig. 1c), which also showed strong blue emission under UV irradiation (Fig. 1d). Furthermore, water is often used to induce organic molecular aggregation for investigating aggregation-induced emission (AIE) or AIEE properties of organic molecules,<sup>20</sup> but there are just few reports on the water molecule-induced assembly of organic molecules.<sup>15</sup> Interestingly, when 1.0 mL

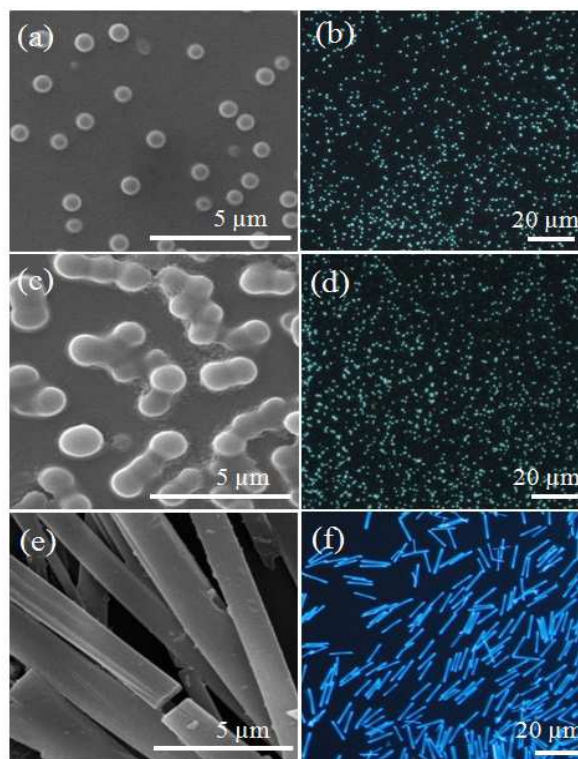
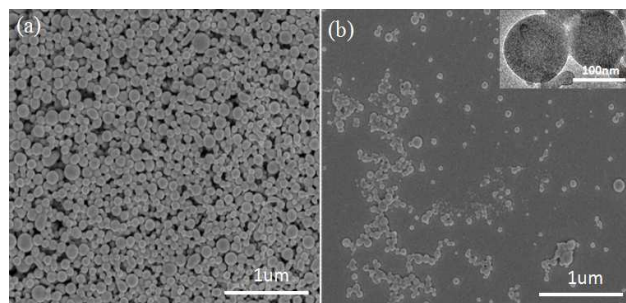


Fig. 1 SEM and FM images of DPCP particles: spheres (a, b), pod-like connecting spheres (c and d) and microrods (e and f) obtained by using DPCP/methanol solution (a-d) and DPCP/methanol-water mixture solution (e and f).

stock of 0.05 mM DPCP/methanol was injected into 4.0 mL of water, the crystallographic microrods with the diameter of 1.0–1.4  $\mu\text{m}$  and the length of more than 5  $\mu\text{m}$  were obtained (Fig. 1e) and the emission of particles was enhanced, as shown in Fig. 1f. Other good solvents were also chosen to dissolve DPCP, such as tetrahydrofuran and ethanol, but no samples with regular morphologies as that prepared from methanol were obtained (Fig. S1).

The surfactants have been widely used to tailor the size and shape of inorganic micro/nanostructure,<sup>21</sup> the usage of surfactants as reaction media to grow organic particles is expected. In our experiments, two surfactants including poly(ethylene glycol)-block-poly(propylene glycol)-block-poly(ethylene glycol) (P123) and hexadecyltrimethylammonium bromide (CTAB) were used to prepare micro/nanostructures of DPCP. 1.0 mL stock of 0.05 mM DPCP/methanol was injected into 4.0 mL of P123 aqueous solution (1 mg/mL) under vigorous stirring, and then the mixture was stirred for 10 minutes and left standing for 5 h for stabilization. After evaporation of the solvents, the nanospheres with 140–170 nm were prepared on a glass-substrate (Fig. 2a), which are smaller than that formed from pure DPCP/methanol solution. Unexpectedly, the smallest nanospheres with 60–120 nm were prepared under the same conditions except P123 was replaced by CTAB (Fig. 2b). This structure was further confirmed by transmission electron microscopy (TEM) (inset in Fig. 2b). These particles also showed blue emission under UV irradiation (Fig. S2). The effect of initial concentration of surfactant on size and morphology was also studied, and obtained particles had only minor changes in the size without obvious modification of the shapes (Fig. S3). The above results demonstrated that the composition solution composition has a significant influence on morphologies of DPCP particles.

To confirm the composition and purity of the obtained samples, the particles were dissolved in  $\text{CD}_2\text{Cl}_2$  and characterized by using  $^1\text{H-NMR}$  and MS ( $\text{ESI}^+$ ). All these spectra are identical to that of the original DPCP, which suggests that prepared micro/nanostructures have the same molecular structure of DPCP. The PXRD was used to further characterize the structures of the as-prepared samples, as shown in Fig. 3 and Fig. S4. PXRD pattern of samples show a broad band peak arising from the poor crystallinity of the samples. No other peak is observed in Fig. 3a, which indicates that obtained nanospheres of DPCP are amorphous or weakly crystalline



**Fig. 2** SEM images of DPCP samples prepared by using different surfactants. (a) P123 and (b) CTAB. Inset is TEM images of spheres.

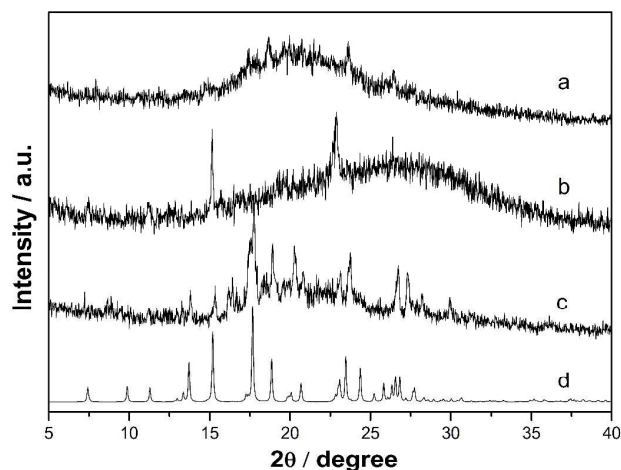


**Fig. 3** PXRD patterns of DPCP with different morphologies. (a) nanospheres, (b) pod-like connecting spheres, (c) microrods and (d) simulated.

materials. The PXRD pattern of pod-like connecting spheres show two sharp peaks at  $15.2^\circ$  and  $22.8^\circ$  ( $2\theta$ ) (Fig. 3b), respectively, indicating a slightly crystalline structure of DPCP molecules in these particles. Furthermore, the PXRD pattern of microrods (Fig. 3c) show sharp and intense peaks which are at the similar positions as those of the stimulated XRD pattern obtained from DPCP single crystal diffraction data (Fig. 3d), indicating that molecular structure of DPCP remains unchanged and microrods are highly crystalline.

The morphology evolution from nanospheres to microrods based on DPCP is remarkable, although the formation mechanism of such particles is not yet clear. For understanding nucleation and growth processes for these particles, the crystal structure of DPCP was successfully solved by single crystal X-ray analysis (Tables S1 and S2). Single crystals of DPCP were obtained by the slow evaporation of their methanol/ $\text{CH}_2\text{Cl}_2$  mixture solution (Fig. S5). DPCP is non-planar and terminal 4-dibenzothiophene has certain distortions from the bulky conjugation skeletons with dihedral angles of  $37.35^\circ$  (Fig. 4a). Two single molecules are packing by aromatic C-H $\cdots$  $\pi$  interactions to form a dimer (Fig. 4b) as X-aggregates<sup>[20b]</sup>

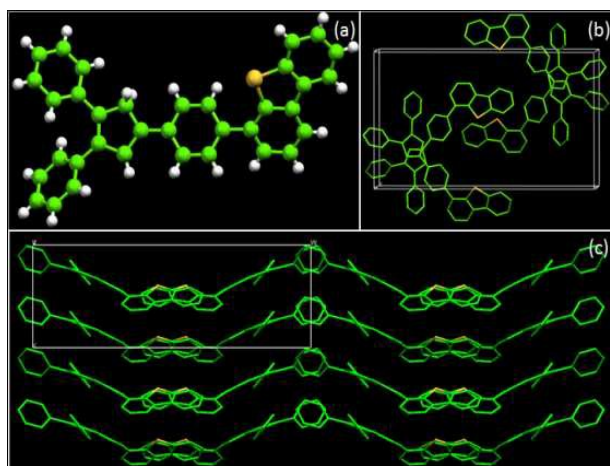
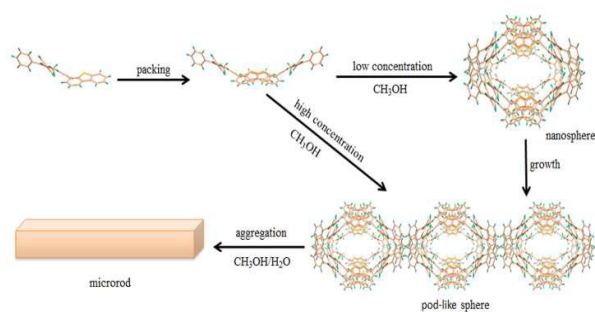


**Fig. 4** Molecular structure (a), dimer structure (b) and packing arrangement (c) in the crystal structure of DPCP.



**Scheme 2** Schematic illustration of the possible growth mechanism for DPCP particles with different morphologies.

which increase the resistance between molecules. Interestingly, the molecules are stacked alternately to form a one-dimensional (1-D) chain along *b*-axis. This structure feature further avoided the maximum face-to-face stacking (Fig. 4c), which further improve the fluorescence intensity in aggregation state. Based on the experimental findings and crystal structure analysis, the proposed assembling mechanism is depicted schematically in scheme 2. The formation of particles with different morphology can be attributed to the solubility controlled crystalline nucleation. When DPCP was dissolved in methanol with lower concentration, twisted molecules prefer to aggregate *via* weak C-H... $\pi$  interactions to form a spherical structure, and the surrounding methanol molecule became the driving force for limiting their further growth.<sup>6</sup> When the concentration of DPCP/methanol solution was increased, more and more nanospheres had the predisposition toward pod-like connecting spheres due to the effect of van der Waals contacts.<sup>2a</sup> When DPCP/methanol solution was injected into water, solvophobic tendency between the DPCP and the water causes supersaturation of DPCP, leading to crystal nucleation and adjusting the orientation during the growth stage. Finally, crystallographic microrods were obtained.

To further investigate formation mechanism of the products, a series of experiments with different DPCP concentrations in methanol/H<sub>2</sub>O mixture solution were carried out. Compared to obtain the monodispersed spheres at low concentration of DPCP (0.01 mM) in methanol (Fig. 1a), pod-like connecting spheres coexist with a small amount of irregular rods under the same concentration in the presence of H<sub>2</sub>O, as shown in Fig. 5a. When the concentration of DPCP was increased to 0.05 mM, microrods became predominate product (Fig. 5b). When the concentration was 0.1 mM and 0.5 mM, microrods with different sized were observed (Figs. 5c and 5d), respectively. According to previous works,<sup>15</sup> the solution compositions had very important effect on microenvironment of organic molecules during self-assembly of micro-/nanostructures. The formation of such different structures might be relative to the amount of free DPCP and crystal seeds in solution. The results indicated that concentration is important kinetically control fact for assembling progress.

In order to understand effects of such different morphologies on photophysical properties, the

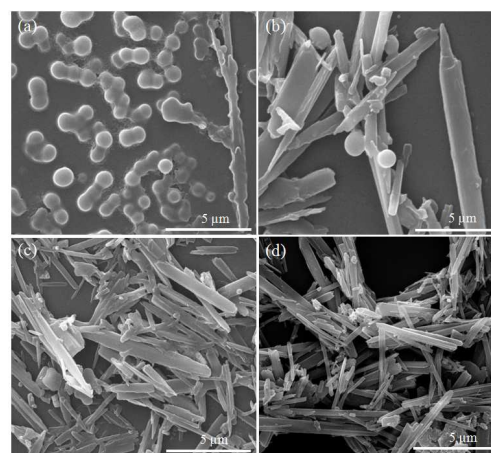


**Fig. 5** SEM images of products synthesized in the presence of H<sub>2</sub>O with different concentrations of DPCP. (a) 0.01 mM, (b) 0.05 mM, (c) 0.1 mM, (d) 0.5 mM.

photoluminescence spectra (PL) of DPCP in solution and at solid state were examined. Interestingly, these structures with different morphologies exhibit distinct fluorescence behaviour. Solution of DPCP in methanol are weaker emission with a peak at 455 nm, however, the nanosphere, pod-like connecting spheres and microrods exhibit remarkably enhanced fluorescence emission with peaks at 447, 448, 468 nm,

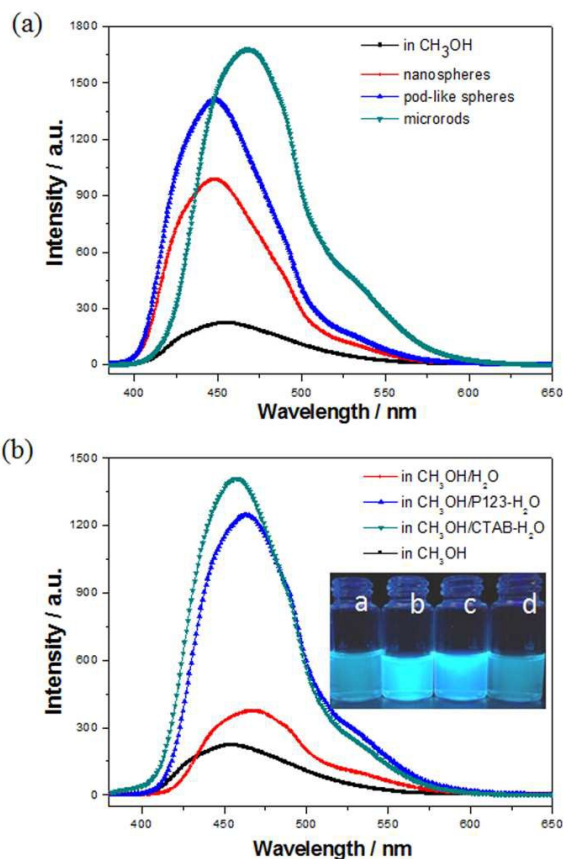


**Fig. 6** photoluminescence spectra of the DPCP in solution (0.01 mM) and at solid state (a) and DPCP particles dispersed in different solution. Inset: fluorescent images of samples under 365 nm UV irradiation.

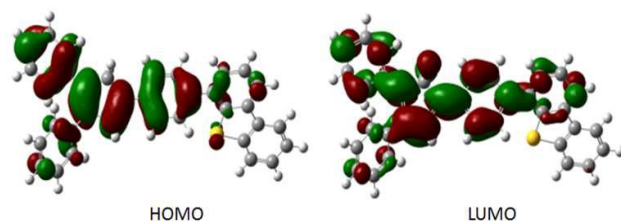


Fig. 7 Calculated molecular orbital amplitude plots of HOMO and LUMO levels of DPCP.

respectively (Fig. 6a). Obviously, the PL spectra of microrods have a red-shift in comparison to that of the original solutions, which may be caused by a water-triggered structural formation.<sup>15</sup> Such enhanced emission could be attributed to the synergetic effect of crystallization effect and restricted intramolecular rotation. Furthermore, there is a shoulder peak in the PL spectra of particles, which might be attributed to the excimer formation by aggregation.<sup>20b</sup> The exact mechanism of the morphology-dependent luminescent properties is not entirely clear, but it should be related to the difference in molecular packing structure and molecular interactions.<sup>14</sup>

To confirm the possible AIEE properties during assembling process, the spectroscopic behaviors with water added into organic solvent were studied. As shown in Fig. S6, the absorptions of DPCP in the water/acetone mixture solution with different volume proportion are different. A level-off tail caused by the formation of aggregates was seen in the visible spectral region when the water fraction was over 50%. The maximum absorption wavelength of DPCP moved to longer wavelength which was the mark of the formation of aggregates.<sup>20</sup> With increasing water contents, the enhanced emissions of DPCP were detected which was interpreted as typical AIEE effect.<sup>22, 23</sup> More interestingly, The PL spectra of particles dispersed in different solution are different (Fig. 6b). It was observed that the fluorescence emission of the samples synthesized in CH<sub>3</sub>OH/CTAB-H<sub>2</sub>O was extremely stronger than that formed from CH<sub>3</sub>OH/P123-H<sub>2</sub>O and CH<sub>3</sub>OH/H<sub>2</sub>O. The fluorescence quantum yields of samples are 14.60% in CH<sub>3</sub>OH, 20.53% in CH<sub>3</sub>OH/H<sub>2</sub>O and 25.74% in CH<sub>3</sub>OH/P123-H<sub>2</sub>O, respectively. This phenomenon could be attributed to small-size effect of nanostructures.<sup>24</sup> Such fluorescent change behavior was further verified by time-resolved emission decay measurements. The fluorescence lifetime curves were illustrated in Fig. S7. The fluorescence lifetime of the DPCP in methanol solution with different concentration (0.01 and 0.05 mM) ranged from 0.06 to 0.10 ns, which meant that concentration had slight effect on fluorescence lifetime. However, the emission lifetime of aggregate formed in methanol/water mixture solution showed a biexponential feature with average lifetime of 0.37 ns. It is probably suggesting that the different structures are responsible for the fluorescence lifetime.

Furthermore, quantum chemistry computation was conducted using the DFT (density functional theory) with B3LYP level and the 6-31G/ basis set on Gaussian 09 program. Fig. 7 shows the optimized geometries and the orbital distributions of the highest occupied molecular orbital (HOMO)

and the lowest unoccupied molecular orbital (LUMO) energy levels of DPMPCP. For HOMO and LUMO levels, the electron clouds are mainly located on the centered five-membered ring and benzene ring on 1- and 2-position of itself, revealing there is no remarkable electron transfer or intermolecular charge-transfer (ICT) transition in the molecule. The enhanced emission of fluorescence DPCP particles should be the result of molecular aggregation.

## Conclusions

In conclusion, the fluorescence organic nanospheres, pod-like connecting spheres and microrods based on 1,2-diphenyl-4-(4-dibenzothiényl)phenyl)-1,3-cyclopentadiene have been successfully grown by simply controlling the solution compositions. DPCP molecules are non-planar and are packing to form a one-dimensional chain, which was responsible for the morphologies and luminescent properties difference. The morphologies and size of DPCP particles can be tuned by varying the concentration of DPCP and the surfactant, respectively. DPCP molecule exhibits aggregation induced emission enhancement property. More importantly, changes in morphologies are accompanied by changes in fluorescence emission. This strategy may provide a useful strategy to tune the morphologies and luminescent properties of organic micro/nanostructures, which could be exploited as building blocks for optoelectronic devices.

## Acknowledgements

This work was supported by the National Natural Science Foundation of China (51003009), the Natural Science Foundation of Liaoning Province (2015020199), the Fundamental Research Funds for the Central Universities of China (DUT14LK32) and the Science and Technology Research Foundation of Education Department of Liaoning Province (L2014033).

## References

- (a) Y. B. Guo, L. Xu, H. B. Liu, Y. J. Li, C. M. Che and Y. L. Li, *Adv. Mater.*, 2015, **27**, 985–1013; (b) Q. H. Cui, Y. S. Zhao and J. N. Yao, *Adv. Mater.*, 2014, **26**, 6852–6870.
- (a) Y. S. Zhao, H. Fu, A. Peng, Y. Ma, Q. Liao and J. Yao, *Acc. Chem. Res.*, 2010, **43**, 409–418; (b) B. Rad, T. K. Haxton, A. Shon, S. H. Shin, S. Whitelam and C. M. Ajo-Franklin, *ACS Nano.*, 2015, **9**, 180–190; (c) B. K. An, S. K. Kwon and S. Y. Park, *Angew. Chem. Int. Ed.*, 2007, **46**, 1978–1982.
- (a) T. Kuykendall, P. Ulrich, S. Aloni and P. D. Yang, *Nat. Mater.*, 2007, **6**, 951–956; (b) Y. Xiao, C. Meng, P. Wang, Y. Ye, H. Yu, S. S. Wang, F. X. Gu, L. Dai and L. M. Tong, *Nano Lett.*, 2011, **11**, 1122–1126.
- (a) M. A. Reed, W. R. Frensley, R. J. Matyi, J. N. Randall and A. C. Seabaugh, *Appl. Phys. Lett.*, 1989, **54**, 1034–1036; (b) J. Feng, D. Zhang, Y. F. Liu, Y. Bai, Q. D. Chen, S. Y. Liu and H. B. Sun, *J. Phys. Chem. C.*, 2010, **114**, 6718–6721; (c) J. Goldberger, A. I. Hochbaum, R. Fan and P. D. Yang, *Nano Letters.*, 2006, **6**, 973–977.

- 5 (a) H. Kasai, H. Kamatani, S. Okada, H. Oikawa, H. Matsuda and H. J. Nakanishi, *Jpn. J. Appl. Phys.*, 1996, **34**, L221–L223; (b) H. Kasai, H. Kamatani, Y. Yoshikawa, S. Okada, H. Oikawa, A. Watanabe, O. Ito and H. Nakanishi, *Chem. Lett.*, 1997, 1181–1182; (c) Y. Komai, H. Kasai, H. Hirakoso, Y. Hakuta, S. Okada, H. Oikawa, T. Adschiri, H. Inomata, K. Arai and H. Nakanishi, *Mol. Cryst. Liq. Cryst.*, 1998, **322**, 167–172.
- 6 (a) Y. S. Zhao, H. Fu, A. Peng, Y. Ma, D. Xiao and J. Yao, *Adv Mater.*, 2008, **20**, 2859–2876; (b) X. Cheng, K. Wang, S. Huang, H.Y. Zhang, H.Y. Zhang and Y. Wang, *Angew. Chem. Int. Ed.*; 2015, **54**, 8369–8373.
- 7 (a) G. Konvalina and H. Haick, *Acc. Chem. Res.*, 2014, **47**, 66–76; (b) N. Chandrasekhar and R. Chandrasekar, *Chem. Commun.*, 2010, **46**, 2915–2917.
- 8 (a) Y. S. Zhao, D. B. Xiao, W. S. Yang, A. D. Peng and J. N. Yao, *Chem. Mater.*, 2006, **18**, 2302–2306; (b) E. M. Garcia-Frutos, *J. Mater. Chem. C*, 2013, **1**, 3633–3645; (c) X. J. Zhang, G. D. Yuan, Q. S. Li, B. Wang, X. H. Zhang, R. Q. Zhang, J. C. Chang, C. S. Lee and S. T. Lee, *Chem. Mater.*, 2008, **20**, 6945–6950; (d) A. Patra, N. Venkatram, D. Narayana Rao and T. P. Radhakrishnan, *J. Phys. Chem. C*, 2008, **112**, 16269–16274; (e) H. Yu and L. M. Qi, *Langmuir*, 2009, **25**, 6781–6786; (f) F. Balzer, M. Schiek, A. Lützen and H. G. Rubahn, *Chem. Mater.*, 2009, **21**, 4759–4767.
- 9 X. H. Sheng, A. Peng, H. B. Fu, Y. Y. Liu, Y. S. Zhao and J. N. Yao, *Nanotechnology*, 2007, **18**, 145707/1–145707/7.
- 10 L. Qian, A. Ahmed and H. Zhang, *Chem. Commun.*, 2011, **47**, 10001–10003.
- 11 W. Xiong, E. U. Athresh, Y. T. Ng, J. Ding, T. Wu and Q. Zhang, *J. Am. Chem. Soc.*, 2013, **135**, 1256–1259.
- 12 (a) Y. S. Zhao, C. Di, W. Yang, G. Yu, Y. Liu and J. Yao, *Adv. Funct. Mater.*, 2006, **16**, 1985–1991; (b) Y. Jia, T. Y. Sun, J. H. Wang, H. Huang, P. Li, X. F. Yu and P. K. Chu, *CrystEngComm*, 2014, **16**, 6141–6148.
- 13 B. Yang, J. C. Xiao, J. I. Wong, J. Guo, Y. C. Wu, L. Ong, L. Lao, F. Boey, H. Zhang, H. Y. Yang and Q. Zhang, *J. Phys. Chem. C*, 2011, **115**, 7924–7927.
- 14 X. J. Zhang, C. P. Zhao, J. Y. Lv, C. Dong, X. M. Ou, X. H. Zhang and S. T. Lee, *Cryst. Growth Des.*, 2011, **11**, 3677–3680.
- 15 F. Zhou, P. L. Tan, Y. Ma, Y. Y. Li, N. J. Li, H. Li, L. H. Wang, H. W. Gu, Q. F. Xu and J. M. Lu, *Chem. Asian J.*, 2014, **9**, 223–228.
- 16 (a) G. L. Ning, X. C. Li, M. Munakata, W. T. Gong, M. Maekawa and T. Kamikawa, *J. Org. Chem.*, 2004, **69**, 1432–1434; (b) X. D. Zhang, J. W. Ye, S. N. Wang, W. T. Gong, Y. Lin and G. L. Ning, *Org. Lett.*, 2011, **13**, 3608–3611; (c) L. J. Yang, J. W. Ye, Y. Gao, D. Deng, Y. Lin and G. L. Ning, *Eur. J. Org. Chem.*, 2014, 515–522.
- 17 (a) L. J. Yang, J. W. Ye, L. F. Xu, X. Y. Yang, W. T. Gong, Y. Lin and G. L. Ning, *RSC Adv.*, 2012, **2**, 11529–11535; (b) X. D. Zhang, J. W. Ye, L. F. Xu, L. J. Yang, D. Deng and G. L. Ning, *J. Lumin.*, 2013, **139**, 28–34; (c) J. W. Ye, D. Deng, Y. Gao, X. X. Wang, L. J. Yang, Y. Lin and G. L. Ning, *Spectrochim. Acta. A. Mol. Biomol. Spectrosc.*, 2015, **134**, 22–27; (d) J. W. Ye, Y. Gao, L. He, T. T. Tan, W. Chen, Y. Liu, Y. Wang and G. L. Ning, *Dyes and Pigments*, 2016, **124**, 145–155.
- 18 (a) B. Yong, S. Zhao, H. Fu, F. Hu, A. D. Peng and J. Yao, *Adv Mater.*, 2007, **973**, 3554–3558; (b) C. Adachi, T. Tsutsui and S. Saito, *Appl. Phys. Lett.*, 1990, **56**, 799–801; (c) X. C. Gao, H. Cao, L. Huang, Y. Y. Huang, B. W. Zhang and C. H. Huang, *Appl. Sur. Sci.*, 2003, **210**, 183–189; (d) Y. Ohmori, Y. Hironaka, M. Yoshida, A. Fujii and K. Yoshino, *Jpn. J. Appl. Phys.*, 1996, **35**, 4105–4109.
- 19 (a) J. Luo, Z. Xie, J. W. Y. Lam, L. Cheng, H. Chen, C. Qiu, H. S. Kwok, X. Zhan, Y. Liu, D. Zhu and B. Tang, *Chem. Commun.*, 2001, 1740–1741; (b) J. W. Ye, L. F. Xu, Y. Gao, H. Wang, Y. Z. Ding, D. Deng, W. T. Gong and G. L. Ning, *Synth. Met.*, 2013, **175**, 170–173.
- 20 (a) F. Wang, M. Han, K. Y. Mya, Y. Wang and Y. Lai, *J. Am. Chem. Soc.*, 2005, **127**, 10350–10355; (b) B. K. An, S. K. Kwon, S. D. Jung and S. Y. Park, *J. Am. Chem. Soc.*, 2002, **124**, 14410–14415.
- 21 Q. Zhang, Y. Divayana, J. Xiao, Z. Wang, E. R. T. Tiekink, H. M. Doung, H. Zhang, F. Boey, X. W. Sun and F. Wudl, *Chem. Eur. J.*, 2010, **16**, 7422–7426.
- 22 (a) Y. Hong, J. W. Y. Lam and B. Z. Tang, *Chem. Commun.*, 2009, 4332–4353; (b) Y. Hong, J. W. Y. Lam and B. Z. Tang, *Chem. Soc. Rev.*, 2011, **40**, 5361–5388.
- 23 (a) J. W. Barr, T. W. Bell, V. J. Catalano, J. I. Cline, D. J. Phillips and R. Procupez, *J. Phys. Chem. A.*, 2005, **109**, 11650–11654; (b) J. Huang, N. Sun, J. Yang, R. Tang, Q. Li, D. Ma and Z. Li, *Adv. Funct. Mater.*, 2014, **24**, 7645–7654; (c) J. Huang, Y. Jiang, J. Yang, R. Tang, N. Xie, Q. Li, H. S. Kwok, B. Tang and Z. Li, *J. Mater. Chem. C*, 2014, **2**, 2028–2036.
- 24 (a) X. H. Liu, Y. S. Wu, S. H. Li, Y. Zhao, C. Q. Yuan, M. Y. Jia, Z. X. Luo, H. B. Fu and J. N. Yao, *RSC Adv.*, 2015, **5**, 30610–30616; (b) H. Fukatsu, M. Kuno, Y. Matsuda and S. Tasaka, *World J. Nano Sci. Eng.*, 2014, **4**, 35–41.

Graphical Abstracts

**Morphology-controlled assembly and enhanced emission of fluorescence in organic nanospheres and microrods based on 1,2-diphenyl-4-(4-dibenzothieryl)phenyl)-1,3-cyclopentadiene**

*Junwei Ye, Xueming Huang, Yuan Gao, Xiaoxiao Wang, Ting Zhen, Yuan Lin, Xin*

*Liu, and Guiling Ning*

